Stitching of off-axis sub-aperture null measurements of an aspheric surface

Chunyu Zhao* and James H. Burge
College of optical Sciences
The University of Arizona
1630 E. University Blvd.
Tucson, AZ 85721

ABSTRACT

Optical testing of a large convex aspheric surface, such as the secondary of a Ritchey-Chretien telescope, can be performed with a Fizeau interferometer that utilizes subaperture aspheric reference plates, each providing a null test of a subaperture of the larger mirror. The subaperture data can be combined or stitched together to create a map of the full surface. The region of the secondary mirror surface under test in each sub-aperture is an off-axis segment of the parent aspheric surface, therefore, the Fizeau reference requires a non-axi-symmetric aspheric surface to match it. Misalignment of the Fizeau reference relative to the parent in each sub-aperture will then result in aberrations in the measurements other than the ordinary terms of piston and tilt. When stitching sub-aperture measurements together, the apparent aberrations due to the null lens misalignment need to be fitted and subtracted. This paper presents an algorithm to perform this particular type of stitching.

Keywords: optical testing, stitching, aspheric optics

1. INTRODUCTION

It is always difficult to interferometrically test a large convex aspheric surface, such as secondary mirrors for Ritchey-Chretien type of telescopes. The main reason is that a high quality reference surface larger than the test surface is needed for the full aperture test of the surface. A few large convex mirrors, both spherical and aspheric, have been tested with full-aperture Fizeau test at the University of Arizona, Steward Observatory Mirror Lab[1]. Diffractive test plates were used as reference surfaces. As the telescope apertures get bigger and bigger, so do the secondary mirrors. Then the full aperture test is simply impossible. A feasible alternative is to test it in sub-apertures with a small reference surface, then stitch them together to get the full surface map. Stitching technique is not new[2-8], yet testing an aspheric convex surface with an aspheric test plate presents new challenges. Besides the usual piston/tip/tilt that need to be fitted over the overlapped area of the adjacent sub-aperture maps, the lateral misalignment of the aspheric test plate introduces other aberration terms which must be fitted as well and removed from the sub-aperture measurement maps. In this paper, we present an algorithm for fitting these lateral misalignment. The algorithm is extended from the one developed by Otsubo, et al[2]. We wrote Matlab code to implement this algorithm. And we used this program to simulate testing a aspheric convex mirror 1.4m in diameter with an aspheric test plate that is the shape of an off-axis segment of the mirror under test. The simulation results are presented.

2. ALGORITHM

When using an interferometer to test a flat in subaperture, then stitch the measurements together to get the full aperture map, only the piston, tip and tilt for each map need to fitted to remove the difference between the adjacent maps in the overlapped area. Otsubo *et al* outlined the theory behind it. As shown in Figure 1, two adjacent sub-aperture measurement over areas A and A' have height of Z_A and $Z_{A'}$, both expressed in global coordinate (x, y). There are relative piston, tip and tilt between these two measurements. In the overlapped area, there exists a right combination of *a*, *b* and *c* that makes the following relationship true:

czhao@optics.arizona.edu ; phone 520-626-6826, fax 520-621-3389

Interferometry XIV: Techniques and Analysis, edited by Joanna Schmit, Katherine Creath, Catherine E. Towers,
Proc. of SPIE Vol. 7063, 706316, (2008) · 0277-786X/08/$18 · doi: 10.1117/12.795094

$$z_{A'}(x,y) = z_A(x,y) + ax + by + c\,. \quad (1)$$

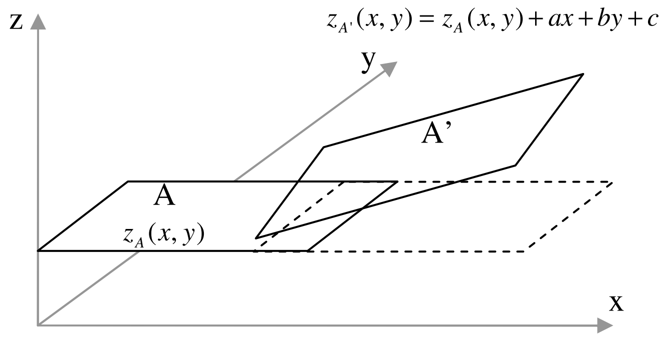

Figure 1. Illustration of piston/tip/tilt between the adjacent subaperture measurements.

Assuming there are N subaperture measurements, and the Nth one is chosen as the reference which does not need to fit, but all other maps have to fit and compensate tip/tilt and piston to minimize the difference over the overlapped area between the adjacent subaperture measurements. For the i-th subaperture map,

$$z'_{i,i\neq N}(x,y) = z_i(x,y) + a_i x + b_i y + c_i\,. \quad (2)$$

The coefficients for tip, tilt and piston for each map, (a_i, b_i, c_i) must be fitted and then compensated to get the full aperture map. Least squared fit is used:

$$\min = \sum_{i=1\ldots N} \sum_{j=1\ldots N}^{j\cap i} \left(\left(Z_i(x,y) + a_i x + b_i y + c_i \right) - \left(Z_j(x,y) + a_j x + b_j y + c_j \right) \right)^2 . \quad (3)$$

The algorithm can be generalized when more terms need to be fitted. The fitting functions for each map may not be limited to tip/tilt and piston. They can be any predefined functions, e.g. they can be arbitrary functions $f_i(x,y)$ where i=1,2,..L, and L is number of functions. Then

$$z'_{i,i\neq N}(x,y) = z_i(x,y) + \sum_{k=1}^{L} F_{ik} f_k(x,y)\,, \quad (4)$$

where coefficients F_{ik} need to be fitted. Again least squared fitting is used:

$$\min = \sum_{i=1\ldots N} \sum_{j=1\ldots N}^{j\cap i} \left(\left(Z_i(x,y) + \sum_{k=1}^{L} F_{ik} f_k(x,y) \right) - \left(Z_j(x,y) + \sum_{k=1}^{L} F_{jk} f_k(x,y) \right) \right)^2 . \quad (5)$$

Eq. (5) can be transformed to a group of linear equations. For the i-th sub-aperture measurement, the fitting coefficients form an Lx1 vector R whose k-th element is F_{ik}, i.e.

$$R_i[k] = F_{ik}\,, \quad (6)$$

For any two subaperture measurements, e.g. the i-th and j-th, we construct an Lx1 vectors P_{ij} and an LxL matrix Q_{ij}, where

$$P_{ij}[k] = \sum_{i\cap j} f_k(x,y) \left(Z_i(x,y) - Z_j(x,y) \right), \quad (7)$$

and

$$Q_{ij}(m,n) = \begin{cases} \sum_{i \cap j} f_m(x,y) f_n(x,y) & i \neq j \\ 0 & i = j \end{cases}, \tag{8}$$

We borrow the concept of cell array from Matlab[9] and make cell arrays **P**, **Q** and **R** which are defined as follows:

1. **P** is a (N-1)x1 cell array whose element is

$$\mathrm{P}\{i,1\} = \sum_{j=1}^{N} p_{ij} \ . \tag{9}$$

2. **Q** is a (N-1)x(N-1)cell array whose element is

$$\mathbf{Q}\{i,j\} = -\delta_{ij} \sum_{k=1}^{N} Q_{ik} + Q_{ij} \ , \tag{10}$$

$$\text{where } \delta_{ij} = \begin{cases} 1 & i = j \\ 0 & i \neq j \end{cases}.$$

3. **R** is a (N-1)x1 cell array whose element is

$$\mathbf{R}\{i,1\} = R_i \ . \tag{11}$$

Note that **P**, **Q** and **R** can be collapsed to regular vectors/matrix with dimensions $((N\text{-}1)\cdot L)$x1, $((N\text{-}1)\cdot L)$x$((N\text{-}1)\cdot L)$ and $((N\text{-}1)\cdot L)$x1, respectively. Then Eq. (5) becomes

$$\mathbf{P} = \mathbf{Q} \cdot \mathbf{R} \ . \tag{12}$$

To solve this in Matlab is straightforward:

$$\mathbf{R} = \mathbf{Q} \backslash \mathbf{P} \ . \tag{13}$$

Now we have obtained the fitting coefficients F_{ik} since they are elements of **R**, then we can combine the subaperture measurements together to get the full aperture map. At the overlapped areas, average is taken over all the subapertures which have valid data over this area. Normal analysis can be performed on the stitched map, such as Zernike decomposition, subtraction of certain reference maps, etc.

A further extension of this approach is that each subaperture map may be fitted to different functions for misalignment. Then P_{ij}, Q_{ij} and R_i are constructed differently, the rest of steps are the same as illustrated above. An example for this application is to test a large convex mirror with two different test plates, each used for different part of the mirror along radial position. Then the lateral misalignment of the test plates will have combinations of different amount of astigmatism and coma.

Assume there are N subaperture measurements, L_i functions denoted as $f_{ik}(x,y)$ need to be fit for the i-th subaperture measurement, and the coefficients are R_{ik}, i.e

$$Z_i(x,y) = Z(x,y) + \sum_{k=1}^{L_i} F_{ik} f_{ik}(x,y) \ , \tag{14}$$

where i = 1, 2, …, N-1 assuming the N-th measurement is used as reference with no-misalignment fitting needed.

Define vector P_{ij} similarly as in Eq. 7, i.e.

$$P_{ij}[k] = \sum_{i \cap j} f_{ik}(x,y) \left(Z_i(x,y) - Z_j(x,y) \right) . \tag{15}$$

Note that in definition described by Eq. 7, P_{ij} and P_{ji} have the same number of elements, and the corresponding elements have the same magnitude but opposite sign. Yet, in the definition for the more general case, there is no such relationship for P_{ij} and P_{ji}. Even the number of elements may be different.

Define vector R_i exactly as in Eq. 6,

$$R_i[k] = F_{ik} \,. \tag{16}$$

Again, R_i and R_j may have different number of elements.

Define Q_{ij} as follows:

$$Q_{ij}(m,n) = \begin{cases} \sum_{i \cap j} f_{im}(x,y) f_{jn}(x,y) & i \neq j \\ -\sum_{k=1\ldots N}^{k \neq i} \sum_{i \cap k} f_{im}(x,y) f_{in}(x,y) & i = j \end{cases} . \tag{17}$$

From the new P_{ij}, and R_i, we can construct the cell arrays **P** and **R** exactly the same as outlined above. But **Q** is a little different,

$$\mathbf{Q}\{i,j\} = Q_{ij} \,. \tag{18}$$

Again, **P**, **Q** and **R** can be collapsed to vectors and matrix, then it is straightforward to get the best fit of the coefficients, F_{ik}, by using Eq. 13.

3. SIMULATION

We implemented in Matlab the simpler version of the algorithm where each subaperture measurement is fitted to the same group of functions. We did a simulation on testing a large convex aspheric mirror with a aspheric test plate. The aspheric test plate is small such that only subaperture measurement can be made on the convex mirror (see Figure 2). The subaperture measurements are arranged such that they cover the whole convex mirror with sufficient overlap between them (see Figure 3). In each subaperture, we need to fit the tip/tilt, piston and power due to the vertical alignment change between subaperture measurements, as well as two other terms that represent the lateral alignment change. The subaperture represents a off-axis portion of the aspheric surface. When the test plate and the mirror under test are both perfect, and perfect null fringe is obtained when they are perfectly aligned. Any lateral misalignment of the test plate in regard to the mirror under test, either a shift along radial direction or clocking or a combination of the two, will produce apparent aberrations which must also be fitted and taken out (see Figure 4).

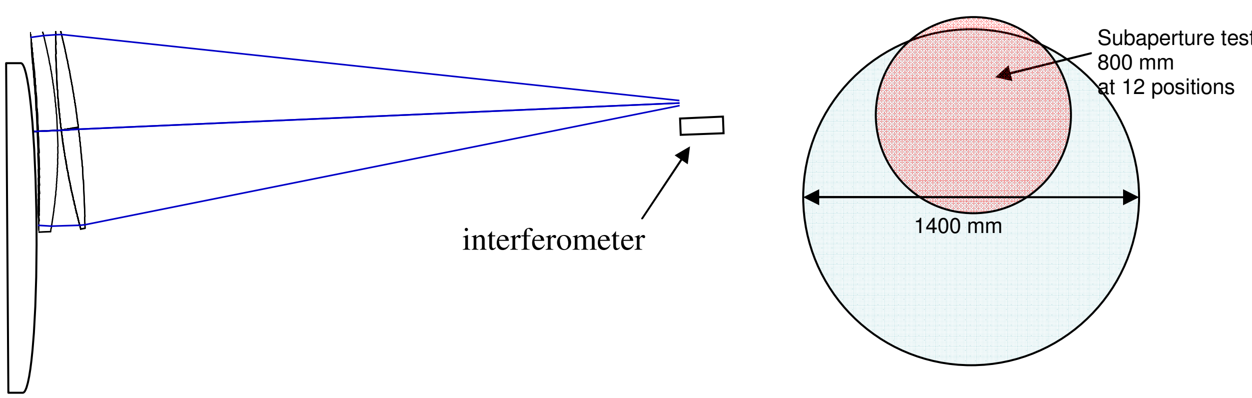

Figure 2. Testing a convex aspheric mirror with smaller test plate. (a) Schematic of test setup. (b) Illustration of full aperture and subaperture relation.

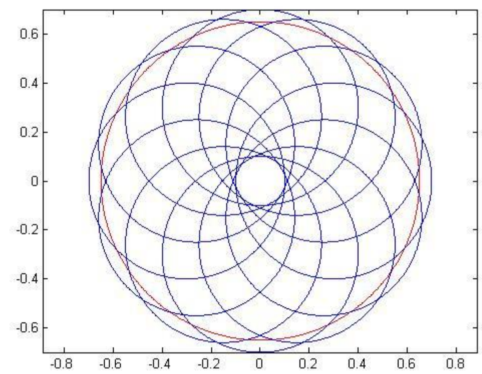

Figure 3. Schematic of the arrangement of the 12 subaperture measurements, 30 degrees apart.

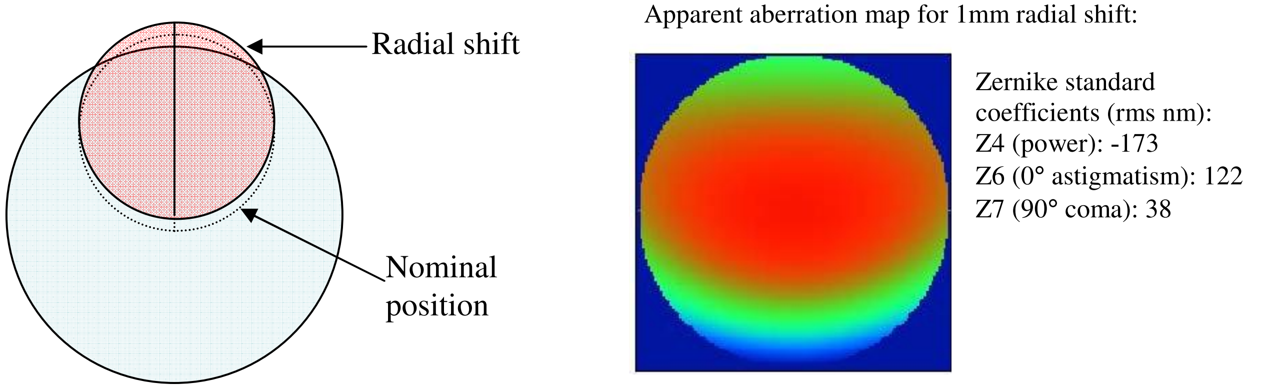

(a)

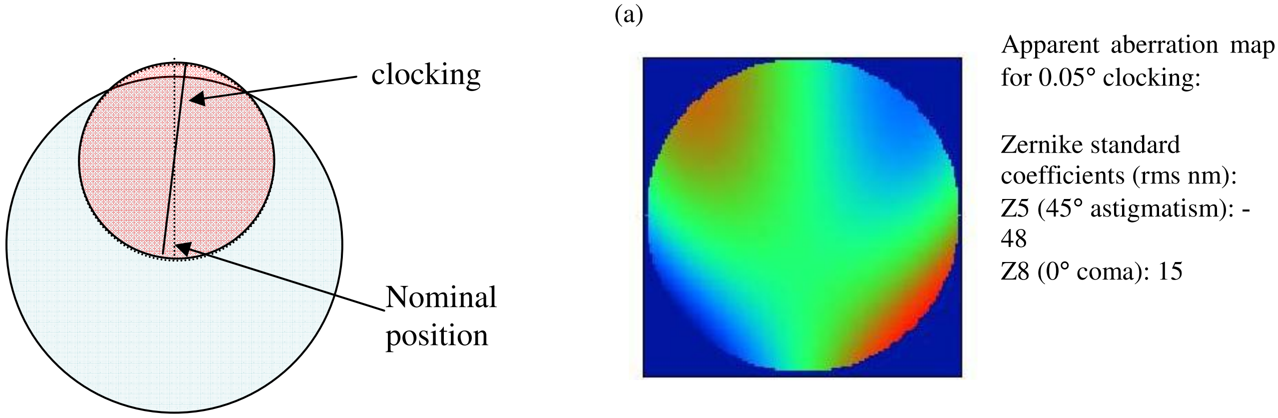

(b)

Figure 4. Illustration of lateral alignment error of the test plate and associated apparent aberration map. (a) radial shift, (b) clocking.

Six functions are fitted for each subaperture measurement to remove the errors caused by misalignment of the test plate relative to the mirror under test. They are listed in Table 1.

Table 1. List of terms fitted for each subaperture measurement.

Term	Expression	Corresponding test plate alignment error
1	$f_1(x, y) = 1$	piston
2	$f_2(x, y) = x$	Tilt in x direction
3	$f_3(x, y) = y$	Tilt in y direction
4	$f_4(x, y) = x^2 + y^2$	Focus error in z
5	$f_5(x, y) = 0.122 \cdot Z6(x, y) + 0.038 \cdot Z7(x, y)$	Radial shift in x-y plane
6	$f_6(x, y) = 0.048 \cdot Z5(x, y) + 0.015 \cdot Z8(x, y)$	Clocking in x-y plane

We simulated testing the mirror in 12 angular positions, 30 degrees apart, as shown in Figure 3. The software is thoroughly tested. When there is only aberrations due to test plate misalignment in each subaperture measurement, the stitching returns a perfect null map of full aperture. We further simulated the noise effect by adding 3nm rms correlated noise to each subaperture map, besides the aberrations caused by random alignment errors. A typical subaperture map is shown in Figure 5. And the result of a typical stitching run is shown in Figure 6.

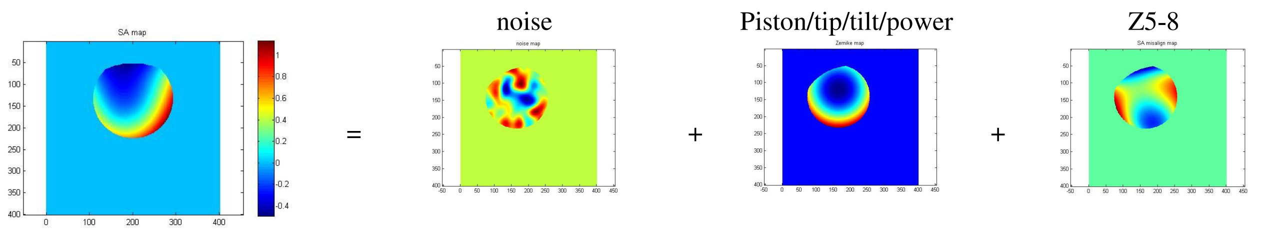

Figure 5. A typical subaperture map is composed of three parts: correlated noise, alignment errors of piston, tip, tilt and power and alignment errors of combinations of astigmatism and coma.

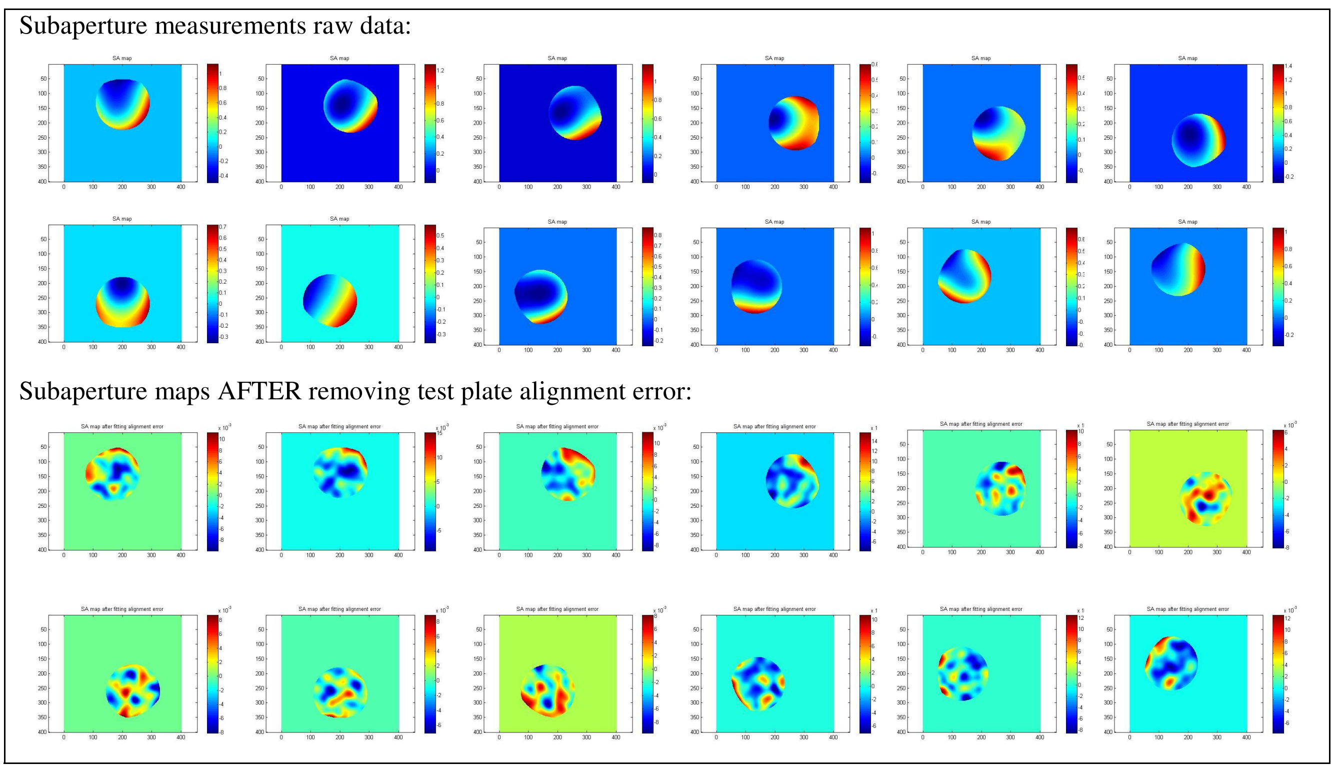

Stitching result:

Stitched map: RMS: 4.1nm | Fitted map: RMS 3.8nm | Residual: RMS: 1.5nm

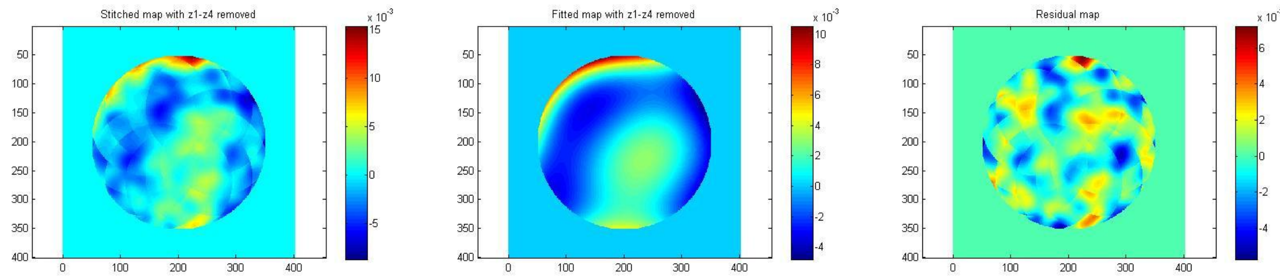

Figure 6. The result of a typical stitching rum.

4. SUMMARY

We generalized a stitching algorithm to deal with cases where, besides the usual tip, tilt and piston terms to be fitted for subaperture measurements, additional terms of virtually arbitrary form need to be fitted as well. We outlined the algorithm in this paper. We also implemented a simpler version in Matlab where each sub-aperture is fitted with the same group of functions. The stitching software we wrote in Matlab was tested extensively and proven to be accurate. We then use it to study testing an aspheric convex mirror in subaperture measurements with a smaller aspheric test plate. The results were presented here. The general version of the stitching algorithm described in Section 2 will be implemented in the near future.

REFERENCES

[1] J. H. Burge, "Fizeau interferometry for large convex surfaces," in *Optical Manufacturing and Testing*, V. J. Doherty and H. P. Stahl, Editors, Proc. SPIE **2536**, 127-138 (1995).

[2] M. Otsubo, K. Okada, J Tsujiuchi, "Measurement of large plane surface shapes by connecting small aperture interferograms," Optical Engineering, **33** (2), 608-613, (1994).

[3] M. Bray, "Stitching interferometer for large plano optics using a standard interferometer", in *Optical Manufacturing and Testing II*, ed. H. P. Stahl, Proc. SPIE **3134**, 39-50. (1997).

[4] S. Tang, "Stitching: High spatial resolution surface measurements over large areas", Proc. SPIE **3479**, 43-49, 1998.

[5] S. Chen, S. Li and Y. Dai, "Iterative algorithm for subaperture stitching interferometry for general surfaces", JOSA A. 22(9), 1929-1936 (2005).

[6] X. Hou, F. Wu, L. Yang and Q. Chen, "Full-aperture wavefront reconstruction from annular sub-aperture interferometric data by use of Zernike annular polynomials and a matrix method for testing large aspheric surfaces", App. Opt. 45(15), 3442-3455 (2006).

[7] P. Murphy, et al, "Stitching interferometer for large plano optics using a standard interferometer", in *Imterferometry XIII: Applications*, ed. E. L. Novak, W. Osten and C. Gorecki, Proc. SPIE **6393**, 62930J, (2006).

[8] C. Zhao, R.A. Sprowl, M. Bray, J.H. Burge, "Figure measurement of a large optical flat with a Fizeau interferometer and stitching technique," in *Interferometry XIII*, edited by E. Novak, W. Osten, C. Gorecki, Proc. of SPIE **6293**, 62930K, (2006).

[9] See Matlab manual or www.mathsoft.com.